



This is a repository copy of *Residence Time Distributions for Turbulent, Critical and Laminar Pipe Flow*.

White Rose Research Online URL for this paper:
<http://eprints.whiterose.ac.uk/94555/>

Version: Accepted Version

Article:

Hart, J.R., Guymer, I., Sonnenwald, F. et al. (1 more author) (2016) Residence Time Distributions for Turbulent, Critical and Laminar Pipe Flow. *Journal of Hydraulic Engineering*, 142 (9). 04016024. ISSN 0733-9429

[https://doi.org/10.1061/\(ASCE\)HY.1943-7900.0001146](https://doi.org/10.1061/(ASCE)HY.1943-7900.0001146)

Reuse

Unless indicated otherwise, fulltext items are protected by copyright with all rights reserved. The copyright exception in section 29 of the Copyright, Designs and Patents Act 1988 allows the making of a single copy solely for the purpose of non-commercial research or private study within the limits of fair dealing. The publisher or other rights-holder may allow further reproduction and re-use of this version - refer to the White Rose Research Online record for this item. Where records identify the publisher as the copyright holder, users can verify any specific terms of use on the publisher's website.

Takedown

If you consider content in White Rose Research Online to be in breach of UK law, please notify us by emailing eprints@whiterose.ac.uk including the URL of the record and the reason for the withdrawal request.



eprints@whiterose.ac.uk
<https://eprints.whiterose.ac.uk/>

Residence Time Distributions for Turbulent, Critical and Laminar Pipe Flow

J. R. Hart, I. Guymer, F. Sonnenwald, and V. R. Stovin

Abstract

Longitudinal dispersion processes are often described by the Advection Dispersion Equation (ADE), which is analogous to Fick's law of diffusion, where the impulse response function of the spatial concentration distribution is assumed to be Gaussian. This paper assesses the validity of the assumption of a Gaussian impulse response function, using Residence Time Distributions (RTDs) obtained from new laboratory data. Measured up- and down-stream temporal concentration profiles have been deconvolved to numerically infer RTDs for a range of turbulent, critical and laminar pipe flows.

It is shown that the Gaussian impulse response function provides a good estimate of the system's mixing characteristics for turbulent and critical flows, and an empirical equation to estimate the dispersion coefficient for Reynolds Number, Re , between 3,000 and 20,000 is presented. For laminar flow, here identified as $Re < 3000$, the RTDs do not conform to the Gaussian assumption due to insufficient time being available for the solute to become cross-sectionally well mixed. For this situation, which occurs commonly in water distribution networks, a theoretical RTD for laminar flow that assumes no radial mixing is shown to provide a good approximation of the system's mixing characteristics at short times after injection.

Introduction

Longitudinal dispersion describes the spreading, relative to the mean flow velocity in the axial direction, of a solute along the longitudinal axis of a flow. Within potable water networks, for example, longitudinal dispersion may affect the concentration/degradation of disinfection chemicals and/or the transport of contaminants. As it is not feasible to continuously monitor or sample water quality throughout a distribution network, it is necessary to be able to predict how the concentration of a solute will change with time (and distance) in the flow (Tzatchkov *et al.*, 2009). Historically, water quality models have assumed steady, highly turbulent flow. This assumption is often valid for the main network, where flow rates are relatively high and steady. However, this assumption does not always hold at the network's periphery. Buchberger *et al.* (2003) show that in the 'dead-end' regions of the network, where water leaves the main network and comes to the point of consumption, flows can be turbulent, critical or laminar. Hence, there is a need to quantify and model dispersion processes for the full range of flow conditions.

Taylor (1953) showed that when a solute is introduced into a flow, after some initial period required for the solute to become cross-sectionally well mixed, equilibrium is obtained between longitudinal differential advection and radial diffusion, at which point the longitudinal distribution of the solute's cross-sectional mean concentration will be Gaussian, with a variance that increases linearly with time. At this point, the process can be described through the Advection Dispersion Equation (ADE), which is analogous to Fick's second law of diffusion:

$$\frac{\partial c}{\partial t} = D_{xx} \frac{\partial^2 c}{\partial x^2} - \bar{u} \frac{\partial c}{\partial x} \quad (1)$$

where c is the cross-sectional mean concentration, t is time; D_{xx} is the longitudinal dispersion coefficient, analogous to Fick's molecular diffusion coefficient, but many orders of magnitude greater, x is distance in the longitudinal direction and \bar{u} is the cross-sectional mean velocity. A standard solution to Equation 1, assuming a Gaussian impulse response function, is:

$$c(x, t) = \frac{M}{A\sqrt{4\pi D_{xx}t}} \exp\left[-\frac{(x-\bar{u}t)^2}{4D_{xx}t}\right] \quad (2)$$

where A and M are cross-sectional area and mass of tracer respectively (Rutherford, 1994).

As longitudinal dispersion is primarily due to differential advection associated with a non-uniform velocity profile, longitudinal dispersion is a function of the flow Reynolds Number, $Re = \bar{u}d/\nu$, where d is the pipe diameter and ν is the fluid's kinematic viscosity. Turbulent flow is generally considered to occur for $Re > 4,000$ (Benedict, 1980). However, more recent work has highlighted that whilst this value is commonly observed in real systems, the exact Reynolds Number at which the transition to turbulence occurs is a function of the conditions of the set-up in question, and thus needs to be measured for a given system (Avila *et al.*, 2011). For fully-developed turbulent flow, the main portion of the velocity profile, deemed the 'turbulent core', is relatively uniform. However, a small portion of the flow near the wall remains laminar, deemed the 'laminar sub-layer', with a 'buffer zone' joining the turbulent core and the laminar sub-layer. Together, the laminar sub-layer and buffer zone form the

boundary layer. The relative portion of the flow made up by the boundary layer increases as Reynolds Number decreases. This change can have an effect on differential advection, as the velocity profile becomes more non-uniform as the relative size of the boundary layer grows.

Hart (2013) showed that for $Re > 20,000$, longitudinal dispersion is small, as the size of the boundary layer is negligible, and thus the near uniform velocity distribution leads to the primary transport mechanism being advection of the solute at the flow's mean velocity. As Re falls below 20,000, the boundary layer starts to form a significant portion of the velocity profile and dispersion tends to increase. For laminar flow, generally considered to occur for $Re < 2,000$ (Benedict, 1980), the velocity has a parabolic distribution which is independent of Reynolds Number and considerably more non-uniform than any profiles typically observed when turbulence is present. Hence, longitudinal dispersion is relatively high for laminar flow. For critical flow, the flow can be either laminar, turbulent or laminar with periods of transient turbulence (Benedict, 1980). Hence, within this range, there is a transition from the relatively low levels of longitudinal dispersion typical for turbulent flow, to the relatively high levels typical for laminar flow. Hart *et al.* (2013) presented initial laboratory results for a single pipe reach and determined longitudinal dispersion coefficients over a range of Reynolds Numbers. The laboratory data clearly showed that the assumption of a Gaussian impulse response function led to increasingly poor fits of the predicted downstream temporal concentration profile to the observed data as Re dropped from 4,000 to 2,000. However, no alternative impulse response function was proposed.

Taylor (1953, 1954) derived expressions to predict the longitudinal dispersion coefficient within fully developed laminar and turbulent pipe flow respectively:

$$D_{xx} = \frac{a^2 \bar{u}^2}{48 D_m} \quad (3)$$

$$D_{xx} = 10.1 a u_* \quad (4)$$

where a is the pipe radius, D_m is the molecular diffusion coefficient and u_* is the frictional velocity.

Fowler and Brown (1943) recorded tracer data, used by Levenspiel (1958), to describe the longitudinal dispersion coefficient for $2,000 < Re < 100,000$. Their measurements were made on 1.5 to 32 m lengths of glass pipe, with radii of 1.58 mm and 3.98 mm. A flow of water was established within the pipe, which was replaced with a salt solution at a given time. A longitudinal dispersion coefficient was obtained by analysing how the leading edge of the salt solution mixed with the trailing edge of the water. Taylor (1954) measured the longitudinal dispersion coefficient using a 16.3 m long stainless steel pipe with an internal radius of 4.77 mm. Salt was injected into the flow of water, and temporal conductivity variations recorded at 3.22 and 16.3 m downstream. Keyes (1955) measured the longitudinal dispersion coefficient in a 2.438 m long glass pipe with an internal radius of 7.75 mm. The longitudinal dispersion coefficient was obtained by measuring the concentration of CO₂ gas injected into air with a thermal conductivity cell. Flint and Eisenklam (1969) measured the longitudinal dispersion coefficient in a 23.45 m long brass pipe with an internal radius of 6.93 13.85 mm. The longitudinal dispersion coefficient was obtained by measuring the concentration of gas injected into oxygen free nitrogen.

Equations 3 and 4 can be used in the ADE (equation 1) to predict the concentration distribution of a solute as it travels through a pipe. However, subsequent work has highlighted two main problems with this approach.

Firstly, neither expression accounts for the trend of the longitudinal dispersion coefficient in the critical zone from turbulent to laminar flow, or for turbulent flow with $Re < 20,000$, where the boundary layer forms a significant portion of the flow (Levenspiel, 1958). Figure 1 shows previously published experimental data from Fowler and Brown (1943), Taylor (1954), Keyes (1955) and Flint and Eisenklam (1969) for the longitudinal dispersion coefficient as a function of Reynolds Number, compared to Taylor's expression for turbulent flow (equation 4). It may be seen that Taylor's (1954) equation increasingly underestimates D_{xx} as Re falls below 20,000.

The second problem with the ADE is that the initial period of mixing within the flow required for the ADE to be valid can be vastly longer than the time scales of interest for e.g. potable water distribution network predictions. For turbulent pipe flow this period is normally negligible, due to rapid radial mixing. Taylor (1954) estimated the distance downstream of an injection for the ADE to be valid for turbulent flow, L , to be:

$$L = 100a \quad (5)$$

This condition corresponds to a time of the order of seconds for fully turbulent flow and typical pipe dimensions. However, for laminar flow, the initial period becomes significant, as the only radial mixing is molecular diffusion,

which is typically several orders of magnitude smaller than turbulent diffusion. Gill and Sankarasubramanian (1970) estimate that for laminar flow, the ADE ‘works well’ for dimensionless mixing times, τ , where:

$$\tau = \frac{D_r t}{a^2} > 0.5 \quad (6)$$

and D_r is the radial diffusion coefficient. Depending on the flow conditions and the pipe diameter, this time can be significant. For example, using Equation 6, Lee (2004) estimated that for a typical North American municipal water main under laminar flow conditions, the period required for the solute to become cross-sectionally well mixed could exceed 2 weeks. Clearly, for most applications, this time period exceeds the time (and distance) scales of interest. A method for predicting the effects of longitudinal dispersion which does not rely on the ADE is required for this initial period.

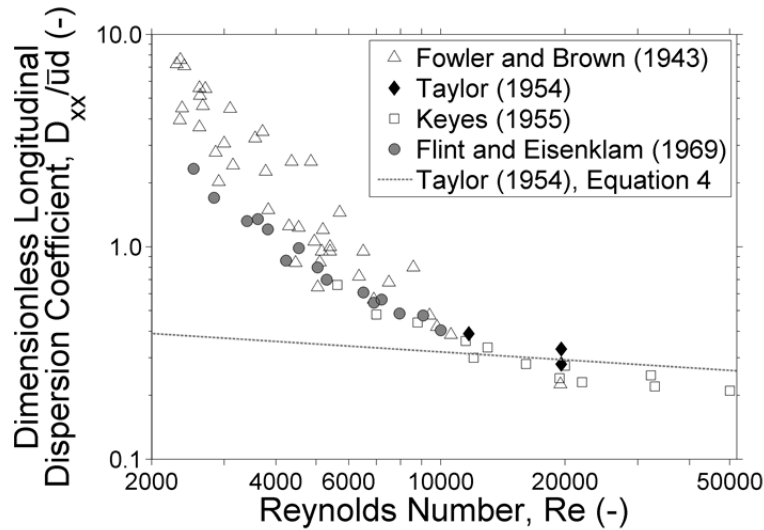


Figure 1 – Comparison between previous experimentally-derived values for the longitudinal dispersion coefficient and the expression of Taylor (1954), as defined in Equation 4

Gill and Sankarasubramanian (1970) showed that the ADE can be ‘useful’ for all times after injection (including $\tau < 0.5$) provided that the longitudinal dispersion coefficient is allowed to vary as a function of time from injection. They derived a time dependent expression for $\tau < 0.5$ that adjusts the magnitude of Taylor’s prediction for laminar flow:

$$D_{xx}(t) = D_m + \frac{a^2 \bar{u}^2}{48 D_m} \left[1 - 768 \sum_{n=1}^{\infty} \frac{J_3(\lambda_n) J_2(\lambda_n)}{\lambda_n^5 [J_0(\lambda_n)]^2} \exp\left(-\lambda_n^2 \frac{D_m t}{a^2}\right) \right] \quad (7)$$

where $D_{xx}(t)$ is the longitudinal dispersion coefficient as a function of time, $J_n(x)$ is a Bessel function of the order n , and λ_n is root of $J_1(x)$. The second term factors Taylor’s longitudinal dispersion coefficient for laminar flow (equation 3). $D_{xx}(t)$ tends towards Taylor’s value as t increases.

Equation (7) is difficult to evaluate, but Lee (2004) showed that it could be approximated to within ‘99.94 %’ by:

$$D_{xx}(t) = \frac{a^2 \bar{u}^2}{48 D_m} \left[1 - \exp\left(-\frac{t}{\tau_0}\right) \right] \quad (8)$$

where $\tau_0 = a^2 / 16 D_m$.

Equation (7) and (8) both quantify the longitudinal dispersion coefficient at an instant in time. To fully describe longitudinal mixing between the point of injection and location or time of interest, equation (8) can be integrated over the duration within the flow. The mean dispersion coefficient, for $\tau < 0.5$, can then be considered:

$$\overline{D}_{xx}(t) = \frac{a^2 \bar{u}^2}{48 D_m} \beta(t) \quad (9)$$

where $\beta(t)$ is a correction factor for Taylor’s prediction for laminar flow. It has been shown by Lee (2004) to perform well for $\tau > 0.01$.

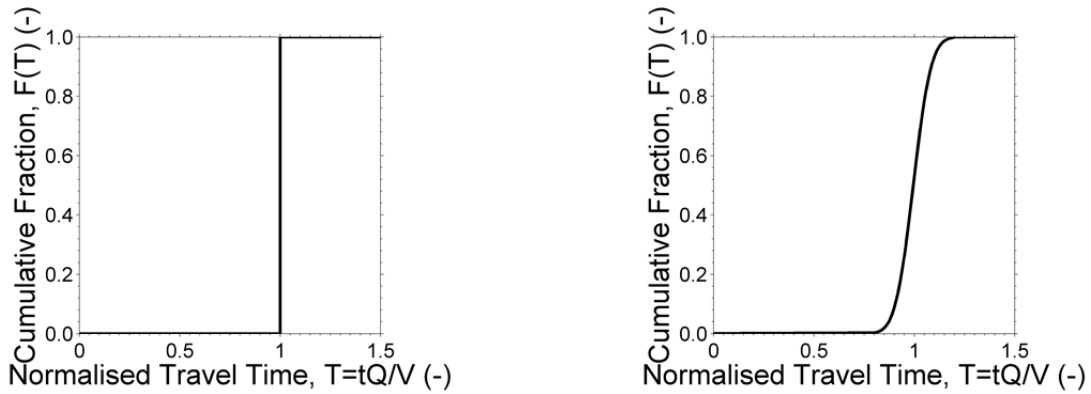
Romero-Gomez and Choi (2011) investigated $\beta(t)$ and discussed Lee’s proposed relationship:

$$\beta(t) = 1 - \exp(-16\tau) \quad (10)$$

They suggested that Lee’s expression performs poorly for very small times after injection ($\tau < 0.01$) where the relationship is ‘quasi-linear’ rather than exponential and found that Lee’s expression produced $\overline{D_{xx}}(t)$ values around 25% greater than experimental and numerical findings. As a result they proposed a new, linear expression for $\beta(t)$ when $\tau < 0.01$, namely:

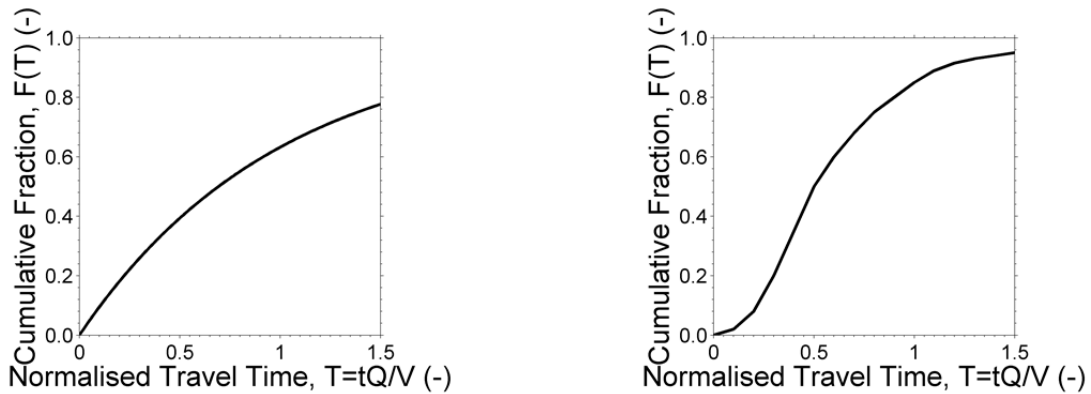
$$\beta(t) = 3.705\tau \tag{11}$$

Danckwerts (1953) suggested an alternative approach to quantifying a system’s mixing characteristics by considering the system’s Residence Time Distribution (RTD). The RTD shows the distribution of times taken by an idealised, instantaneous injection of tracer to exit a system, and thus quantifies the fundamental mixing response of that system. As such, the RTD makes no assumptions about the mixing characteristics of the system. Figure 2 shows Cumulative Residence Time Distributions (CRTDs), the integral form of the RTD, for a variety of systems. The mixing characteristics of most real world systems can be explained as either one or a combination of the regimes proposed in Figure 2. Mixing case (b) is analogous to turbulent pipe flow.



a) Piston Flow

b) Piston Flow with some Longitudinal Mixing



c) Complete Mixing

d) Dead Water

Figure 2 – Example CRTDs (or F-diagrams) for four fundamental mixing regimes (after Danckwerts, 1953)

Danckwerts (1953) derived the following expression for the CRTD for laminar flow simply on the basis of differential advection due to a parabolic laminar velocity profile, neglecting radial exchange altogether:

$$F(T) = 1 - \frac{1}{4T^2} \tag{12}$$

where $F(T)$ is the non-dimensional CRTD, for the normalised travel time, $T = tQ/V$, Q is the volumetric discharge and V is the volume of the system. Figure 3 shows the CRTD produced from Equation 12, for $T > 0.5$, compared with a CRTD for turbulent pipe flow, a cumulative Gaussian impulse response function.

The mixing response of a system can be experimentally investigated by injecting a tracer into a flow and measuring its temporal concentration distribution at up- and down-stream locations. However, recovering the

fundamental mixing response (i.e. the RTD) from this data is non-trivial. This is because the RTD, by definition, shows the system's mixing response to an idealised, instantaneous injection. It is difficult to produce this scenario in a laboratory as the requirement for full cross-sectional mixing typically requires the injection to occur some distance upstream from the upstream monitoring position.

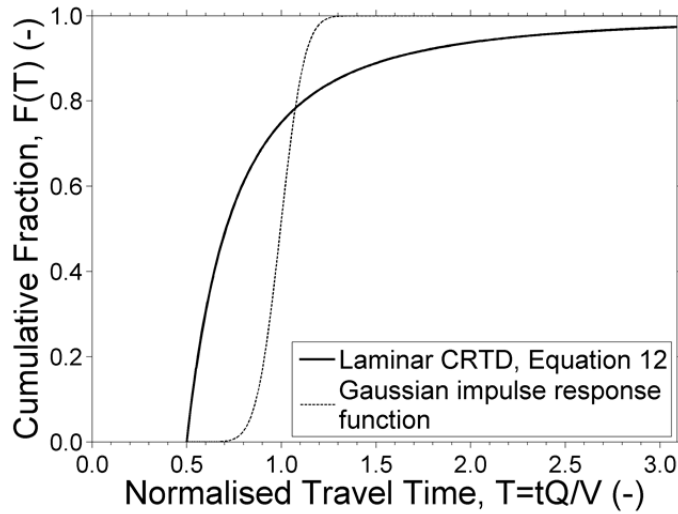


Figure 3 – Theoretical CRTDs for laminar flow and turbulent pipe flow (after Danckwerts, 1953)

Recent work has investigated techniques for recovering the RTD numerically through identification of the impulse response function required to transform a measured upstream profile into a measured downstream profile. Stovin *et al.* (2010) and Guymer and Stovin (2011) used deconvolution (see later section) to recover RTDs from laboratory data from a surcharged manhole. In this case, the mixing processes of interest were generated by the manhole geometry and associated flow-fields. However, to the authors' knowledge, no comparable studies have been conducted for fully-developed pipe flow. Pipe flow is of particular interest, as it represents a 'fundamental' case, where the only mixing mechanisms are generated by the interaction of the flow with the boundary and exchanges generated by molecular and turbulent diffusion. The system's geometry is axis-symmetrical, thus essentially 1D for fully developed flow.

The aim of this study is to characterise the fundamental mixing response of a pipe flow system for the range of Reynolds Number $2,000 < Re < 50,000$, i.e. turbulent, critical and laminar flow. The novelty of the present approach is that it is the first to apply deconvolution to obtain RTDs from laboratory pipe data. Specific objectives are:

- (i) To determine the lower limit of Reynolds Number for which the assumption of a Gaussian impulse response function is valid;
- (ii) If the lower limit of Reynolds Number identified in (i) is significantly below $Re = 20,000$, i.e. in the region where equation 4 is known to be invalid, to identify a practical means of estimating dispersion coefficient to be used in conjunction with the ADE;
- (iii) To assess the validity of Equation 12 (Danckwerts, 1953) for estimating longitudinal mixing in pipes under laminar conditions, and to identify the upper limit of Reynolds Number for which this is applicable, prior to fully mixed conditions, when the dimensionless mixing time, $\tau < 0.5$.

Deconvolution

The relationship between a measured up- and down-stream concentration distribution and the system's RTD is given through the convolution integral:

$$c(x_2, t) = \int_0^t c(x_1, t - \xi) E(\xi) d\xi \quad (13)$$

where $c(x_1, t)$ and $c(x_2, t)$ are the up- and down-stream concentration distributions respectively, $E(\xi)$ is the system's RTD and ξ is an integration variable.

If the up- and down-stream concentration profiles are measured, the data can be deconvolved to give the system's RTD. Madden *et al.* (1996) undertook a comparison of six possible deconvolution techniques for solving Equation 13. Of the six approaches, they concluded that the best in terms of overall performance was 'maximum entropy deconvolution', developed by Skilling and Bryan (1982). Stovin *et al.* (2010) and Guymer and

Stovin (2011) successfully applied maximum entropy deconvolution to data from tracer studies within surcharged manholes.

Sonnenwald *et al.* (2014) further investigated maximum entropy deconvolution and found it to be applicable to a wide range of field and laboratory solute transport data. Their implementation, used in this paper, was based upon Hattersley *et al.* (2008), where maximum entropy deconvolution works through an entropy function to make the RTD smooth while simultaneously constraining it to predict the downstream data. The MATLAB *fmincon* non-linear optimisation function is used to minimise the following set of equations:

$$S(\hat{E}) = - \sum_{i=1}^N \left(\frac{\hat{E}_i}{\sum_{j=1}^N \hat{E}_j} \right) \ln \left(\frac{\hat{E}_i / \sum_{j=1}^N \hat{E}_j}{r_i} \right) \quad (14)$$

$$C = \frac{\sum_{i=1}^N (\hat{y}_i - y_i)^2}{\sum_{i=1}^N y_i^2} \quad (15)$$

$$L(\hat{E}, \lambda) = C + \lambda S(\hat{E}) \quad (16)$$

where \hat{E} is the estimated RTD, N is the number of sample points in the RTD, r is a next-neighbour moving average of \hat{E} , C is an R_t^2 (Young *et al.*, 1980) based function, \hat{y}_i is the predicted downstream concentration distribution (obtained through Equation 13), y_i is the measured downstream concentration distribution, L is the Lagrangian function, and λ is the Lagrange multiplier as determined by a gradient descent method during *fmincon* optimisation (MATLAB). Sonnenwald *et al.* (2014) identified and undertook a sensitivity analysis of four main parameters affecting the maximum entropy deconvolution process as applied to solute transport data: number of sample points, constraint function, number of iterations, and sample point spacing. Their recommendations of 40 sample points, the R_t^2 based constraint function, 350 iterations, and ‘‘Slope Based’’ sub-sampling have been adopted here.

Experimental Methodology

Experimental work was undertaken on a recirculating pipe system with a test section consisting of a 16.56 m long Perspex pipe, with an internal radius of 12 mm. The pipe diameter was the maximum which could pass through the fluorimeters without modification, to permit non-intrusive concentration measurements. Water was re-circulated from a 2500 litre sump. Figure 4 shows a schematic of the experimental setup.

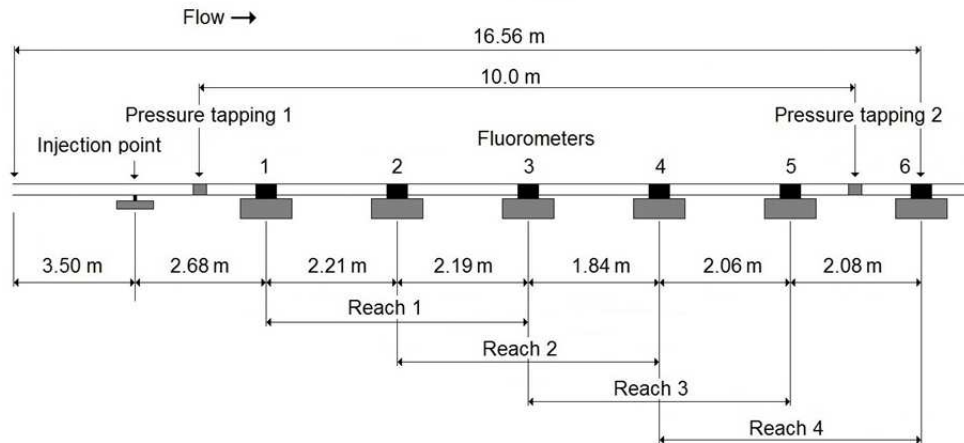


Figure 4 – Experimental test section

The aim of the test series was to measure the system mixing characteristics for $2,000 < Re < 50,000$. A fluorescent dye, Rhodamine WT, was injected into the flow using a computer-controlled peristaltic pump at a distance 3.5 m downstream from the start of the test section, a length estimated as being sufficient for the flow to be fully developed (White, 2011). The first fluorometer was located 2.68 m downstream from the injection point. Dye injections of 1 s duration, at concentrations between 500 – 1500 ppb, were used depending on the flow rate. Cross-sectional average temporal concentration profiles of the dye were recorded using six Turner Designs Series 10 fluorimeters (see Figure 4 for locations). The instruments were calibrated before and after the full series of dye injections to confirm that the calibration relationship had remained constant. The tracer tests investigated 19 Reynolds Numbers between $2,000 < Re < 50,000$. In total 57 tests were conducted with three repeat tests at each discharge. A diffuser was fitted to the sump to stop short circuiting between the outlet and inlet pipes, and the combination of this and the relatively small amount of dye injected for each run compared to the large sump volume meant that no secondary recirculations of dye or measurable increase in

background concentration occurred. Discharge was measured volumetrically 3 times before and after each test to confirm that the flow rate remained constant throughout the test.

Figure 5 shows an example of the recorded concentration profiles above background, showing decreasing peak concentrations and increasing spread with distance along the pipe.

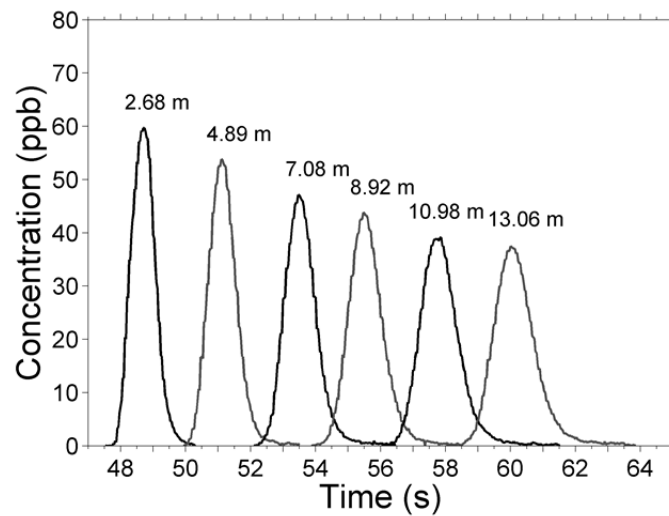


Figure 5 – Example traces showing concentration profiles at each instrument for $Re = 20,500$. Distances given refer to the distance from the injection point.

Figure 6 shows the mean value of mass recovery for the three repeat tests conducted at each Reynolds Number, \pm one standard deviation for each parameter. The mean recovery for all runs undertaken was 98.5 %, with a standard deviation of 9.6%. Figure 6 shows that a mass recovery of around 100%, with relatively low scatter is maintained for $6,000 < Re < 50,000$. However, for $Re < 6,000$, the scatter in the data increases to approximately $\pm 10-15\%$. The errors in mass balance for $Re < 6,000$ are thought to be due to the tracer not being fully cross-sectionally well mixed for critical and laminar flows, as the radial exchange due to turbulence is reduced.

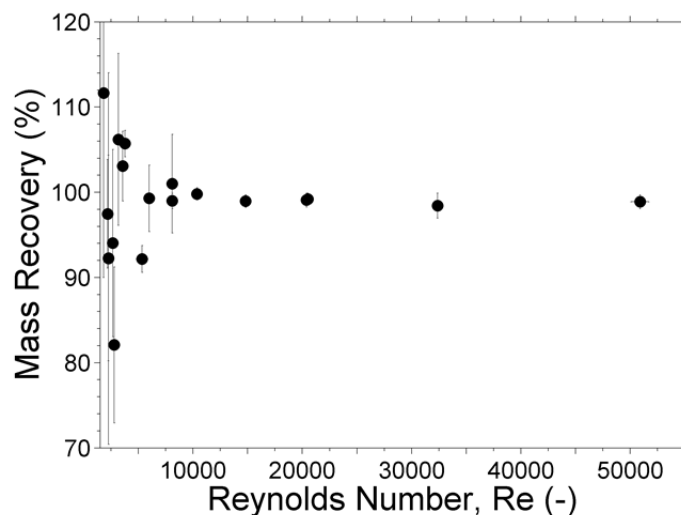


Figure 6 – Variation of mass recovery with Reynolds Number

White (2011) states that the threshold for laminar/critical flow is $Re = 2,300$, whereas Benedict (1980) gives it as $Re = 2,000$. To characterise the hydraulic regime of this specific system, head loss was measured between 2 manometers 10 m apart. The manometers enabled the static head to be measured to the nearest mm. For a given discharge, the static head from the up- and the down-stream manometers was recorded 5 times for each run, and the head loss was calculated as the difference between the mean values of the up- and down-stream

values. Head loss measurements were made for more than 50 different discharges between $2,000 < Re < 50,000$, to provide greater resolution than obtained for the dispersion studies.

Results

Hydraulic Characteristics

The main aim of the experimental programme was to obtain RTDs for a range of Reynolds Numbers covering turbulent, critical and laminar flow. To aid in interpreting the tracer data, initial tests were conducted to characterise the hydraulic regime. Head loss measurements were used to obtain the friction factor using the Darcy-Weisbach Equation (Benedict, 1980):

$$f = h_f \left(\frac{d}{L} \right) \left(\frac{2g}{\bar{u}^2} \right) \quad (17)$$

where f is the friction factor, h_f is head loss, L is the pipe length and g is acceleration due to gravity.

Figure 7 shows this data, in the form of a Moody-style plot (Moody and Princeton, 1944). A simple qualitative assessment of Figure 7, on the basis of standard laminar/turbulent pipe flow theory (Benedict, 1980), suggests that for this specific system the flow is turbulent for $Re > 5,000$, laminar for $Re < 3,000$, and critical for $3,000 < Re < 5,000$.

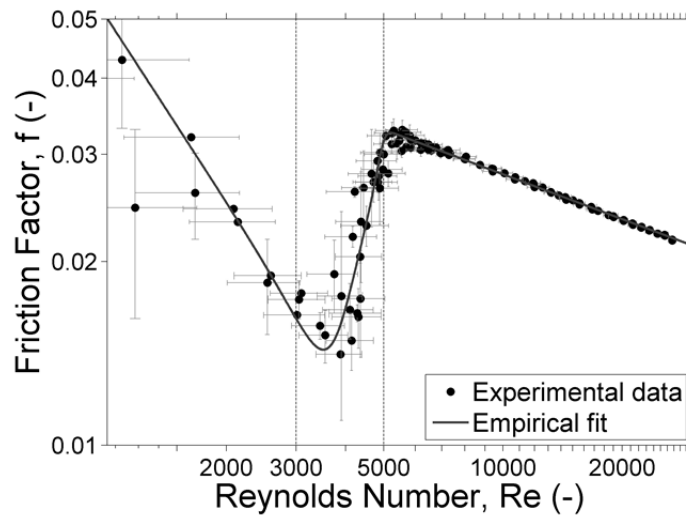


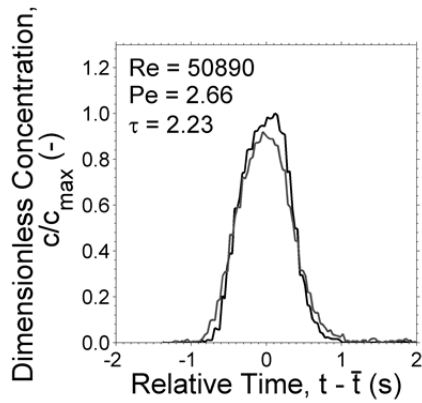
Figure 7 – Variation of friction factor with Reynolds Number

Solute Transport Characteristics

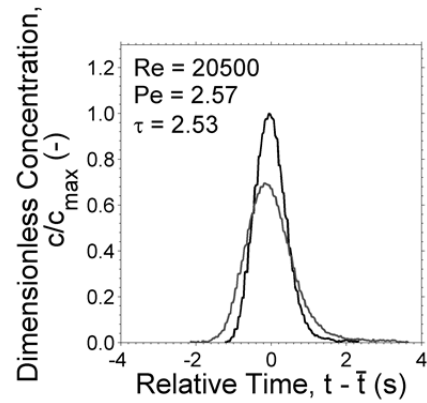
Figure 8 provides example plots of the raw tracer data between the 2nd and final fluorometer for six different values of Reynolds Number. The plots show concentration, normalised with respect to the peak upstream concentration, and with the time axis set so that each profile's centroid corresponds to zero. Values of the Reynolds Number, Re , the Péclet Number, i.e. the ratio of advective to diffusive transport, $Pe = \bar{u}d/D_{xx}$, and the dimensionless mixing time, τ have been provided for reference. Note that in calculating the dimensionless mixing time (equation 6), the value for the radial diffusion coefficient, D_r has been taken as the molecular diffusion coefficient, D_m when $Re < 3,000$ and a value of D_t calculated from Taylor (1954) for critical and turbulent flows, when $Re > 3,000$.

From Figure 8(a) it can be seen that for $Re \approx 50,000$, where the flow is highly turbulent, the profiles are almost symmetrical, with little measurable dispersion occurring between the up- and down-stream locations. From Figure 8(b)-(f), as Reynolds Number decreases, the profiles become increasingly asymmetrical and dispersion increases.

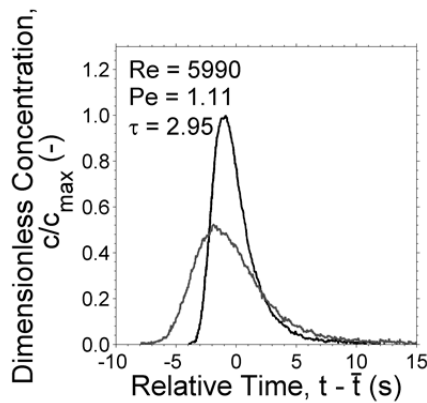
A best-fit longitudinal dispersion coefficient was determined for each test case using an ADE routing procedure (Fischer, 1973). These were used in quantifying the Péclet Number and are presented in Figure 9. Figure 9 confirms that the fitted longitudinal dispersion coefficients are comparable with previous results, shown in Figure 1. At the higher Reynolds Numbers ($Re > 10,000$) the present data appears to overestimate dispersion by a factor of two compared with previous laboratory observations.



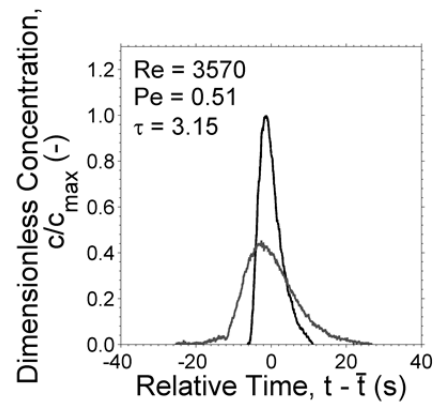
a



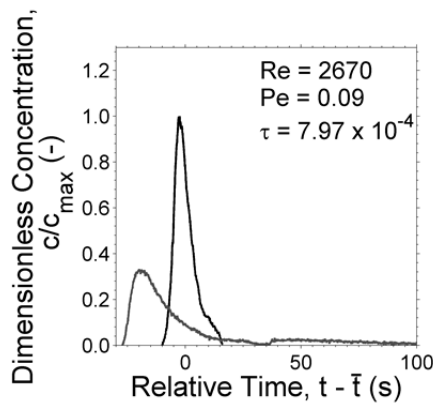
b



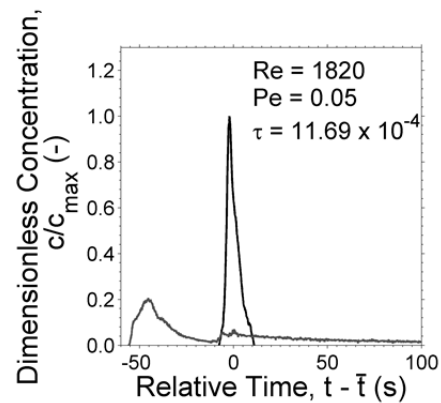
c



d



e



f

Figure 8 – Up- (black) and down-stream (grey) concentration profiles for selected Reynolds Numbers

To obtain the system's fundamental mixing response (RTD), the laboratory data was deconvolved using the maximum entropy deconvolution technique and parameters described previously. Figure 10 shows the CRTDs corresponding to the trace data shown in Figure 8, and compares them with the CRTDs which would result from the combination of the ADE and the relevant fitted dispersion coefficients. Thus, Figure 10 compares the experimentally-obtained actual response of the system with the inferred response assuming the mixing characteristics were a Gaussian impulse response. The goodness of fit between the two CRTDs was quantified using the coefficient of determination, R^2 . For $3,000 < Re < 50,000$ (data shown in Figure 8(a)-(d)), the system's mixing characteristics are generally approximated well (typical values of $R^2 > 0.99$) by a Gaussian impulse response function, with the exception of the profile's trailing edge, which is slightly elongated. However, for $Re <$

3,000 (data shown in Figure 8 (e)-(f)), a change in the system's mixing characteristics occurs, and the fit between the CRTD and a Gaussian response becomes poor ($R^2 < 0.90$).

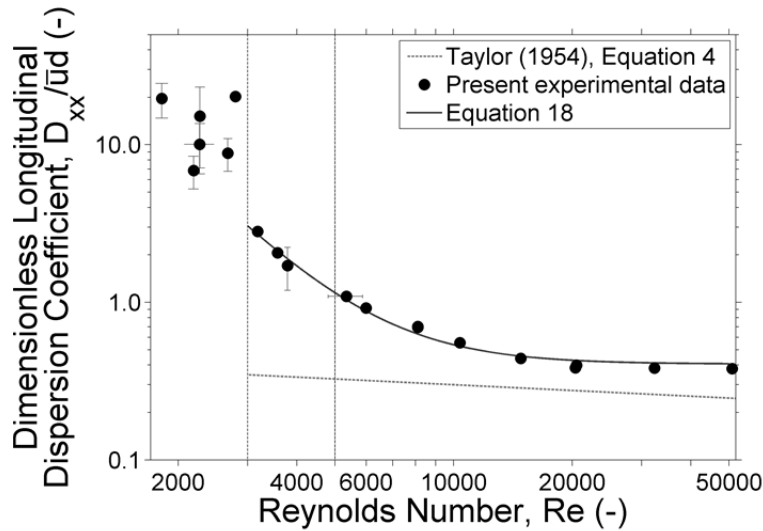


Figure 9 – Longitudinal dispersion coefficients derived from the present experimental data and proposed empirical equation for $3,000 < Re < 50,000$

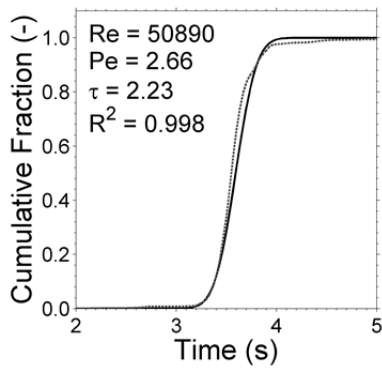
The data in Figure 10 corresponds to a reach that spans almost the entire test section. However, to explore the temporal development of the impulse response function, the system's CRTDs were compared to a Gaussian impulse response function for 4 sub-reaches, where the distance between the up- and the down-stream fluorometers was approximately constant (4 m), but the distance from the injection point to the start of the reach varied. Figure 4 shows the positions of the fluorometers on the test pipe, where Reach 1 is between instruments 1 and 3, Reach 2 instruments 2 and 4, Reach 3 instruments 3 and 5 and Reach 4 instruments 4 and 6.

Table 1 provides examples of the time the tracer would have been in the flow when it arrived at the start of each reach, as well as an estimate of the time required for the tracer to become well-mixed. For $Re \geq 5,000$, the estimate of the time required for the tracer to be well-mixed is made on the assumption that the flow is turbulent, whereas for $Re \leq 3,000$, the calculation assumes laminar flow. It should be noted that for $Re \leq 3,000$, the time in the flow (even for the furthest reach) is three orders of magnitude less than the time required to be well-mixed, whereas for $Re \geq 5,000$, the time in the flow always exceeds the time required to be well-mixed. As described above, this is due to the different magnitudes of radial diffusion.

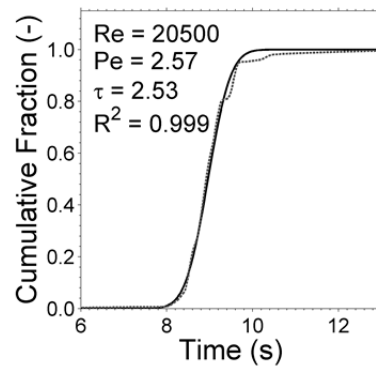
Reynolds Number	50,000	5,000	3,000	2,000
Time to start of Reach 1 (s)	1.1	11.4	18.9	28.4
Time to start of Reach 2 (s)	2.0	20.8	34.6	51.9
Time to start of Reach 3 (s)	3.0	30.1	50.1	75.2
Time to start of Reach 4 (s)	3.8	37.9	63.2	94.7
Estimated time to well-mixed (s)	0.77	5.75	40.8×10^3	40.8×10^3

Table 1: Summary of times solute has been in the flow for each reach

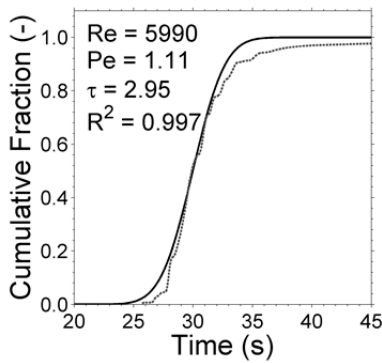
Figure 11 shows the values of R^2 for the comparison between the CRTDs and a Gaussian impulse response function for each of the 57 runs for Reaches 1-4. When $Re > 3,000$, the system's mixing characteristics are described well by a Gaussian impulse response function ($R^2 > 0.95$). This is due to the presence of fully developed turbulence, which leads to the tracer becoming rapidly well mixed. It was anticipated that for critical flow, the system would not be adequately described by a Gaussian impulse response function, although it should conform increasingly better to the Gaussian impulse response function with more time in the flow. In fact, it was observed that for critical flow ($Re > 3,000$), the system conformed to a Gaussian impulse response function for all reaches. It may be inferred that the intermittent turbulent bursts present in critical flow are sufficient to mix the tracer rapidly.



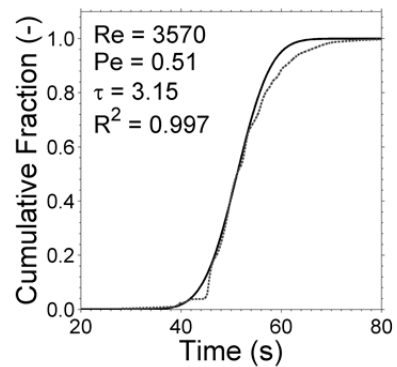
a



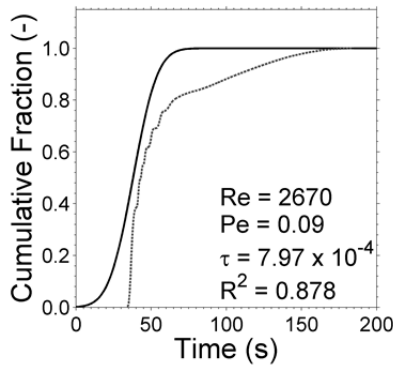
b



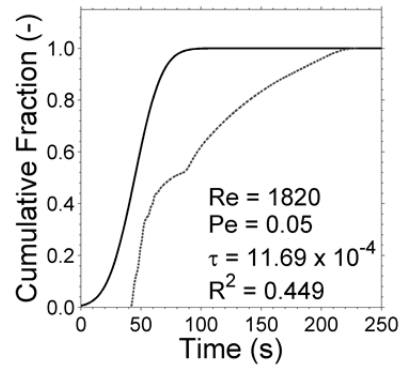
c



d



e



f

Figure 10 – Comparison between deconvolved CRTDs (dashed) and best-fit ADE CRTDs (solid)

However, under laminar conditions ($Re < 3,000$), none of the reach lengths is well described by the Gaussian impulse response function, and there is no observable increase in conformity with increasing time in the flow. On the contrary, the data appears to suggest better conformity with a Gaussian impulse response function for shorter times in the flow. There is not sufficient data to conclusively demonstrate why this might be the case. This may be because the concentration profile immediately after an instantaneous injection is Gaussian in form, only subsequently modifying to reflect the laminar flow conditions. It may also reflect the fact that all the reaches considered here are extremely short relative to the expected distance/time required to achieve full mixing.

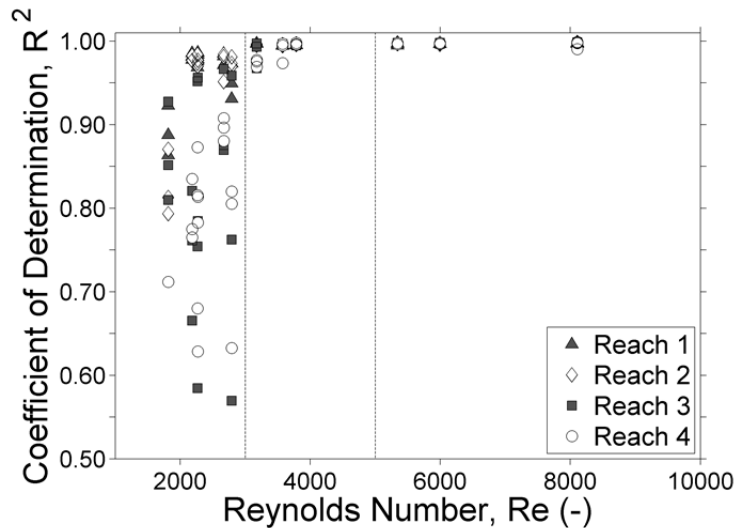


Figure 11 – Correlation between deconvolved CRTDs and best-fit ADE CRTDs as a function of Reynolds Number

Figure 12 provides a comparison between the CRTDs for all Reynolds Numbers in the test series, where each CRTD is the mean profile from three repeats. Here, the up- and down-stream profiles are taken from the 2nd and final fluorometers respectively. The CRTDs are plotted against normalised travel time, $T = tQ/V$. The data has been sub-divided into Reynolds Number bands, and clearly demonstrates the switch between the two main mixing regimes at $Re \approx 3000$.

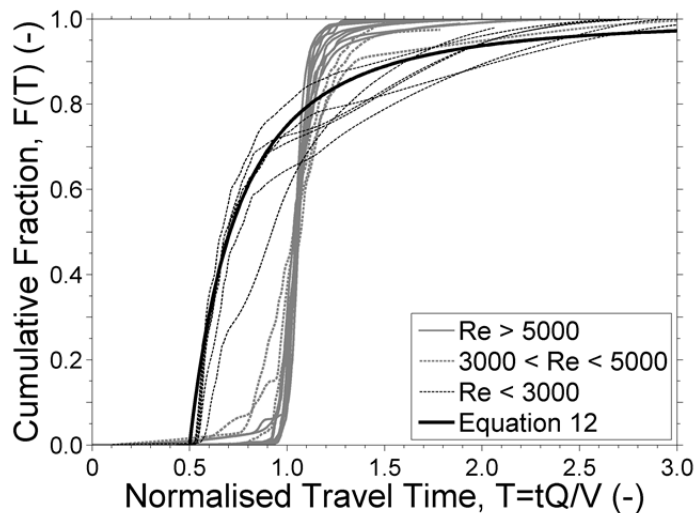


Figure 12 – Dimensionless CRTDs for the entire experimental data set and Danckwerts (1953) CRTD for laminar flow

Discussion

Mixing Regimes

Comparing the CRTDs from Figure 12 with the mixing regimes proposed by Danckwerts (1953), as shown in Figure 2, it may be seen that for $Re > 3000$, the system is conforming to 'piston flow with some longitudinal mixing', i.e. flow is turbulent, but with some longitudinal dispersion occurring due to velocity shear. This type of mixing can be approximated well by a Gaussian impulse response function, as first proposed by Taylor (1954), at relatively short times after injection. Below this threshold, for laminar flow, the distribution of the CRTDs show some similarity to what Danckwerts deemed 'Dead-water', where the high variation in the velocities across a parabolic laminar velocity profile causes some parcels of tracer to get caught near the wall whilst others are transported quickly at the centreline.

The degree to which the flow profile for a particular regime affects solute transport is also highlighted by considering the first arrival of the tracer with respect to the centroid of the CRTD. For plug flow, the first arrival time would correspond to the mean velocity, i.e. $T = 1$. For a non-uniform velocity profile, the first arrival should correspond to the value of the mean to maximum velocity ratio. From Figure 12 it can be seen that for $Re < 3,000$, the first arrival time is around $T \approx 0.5$. This corresponds to the mean to maximum velocity ratio for laminar flow with a parabolic velocity profile, which can be shown analytically to be 0.5. For $Re > 3,000$, the first arrival time is around $T \approx 0.8$. Again, this corresponds to typically observed mean to maximum velocity ratio for turbulent flow (Benedict, 1980). It is evident that Equation 12 is a good representation for $Re > 3,000$, the laminar flow profiles.

The solute transport experiments suggest that the threshold between laminar and non-laminar conditions for this system occurs at $Re \approx 3,000$. However, it should be recalled that the data presented in Figure 7 led to the suggestion that laminar flow extended up to a Re of between 3,000 and 4,000. Whilst it may be inferred that the intermittent turbulent bursts present in critical flow are sufficient to rapidly cross-sectionally mix the tracer, these turbulent bursts are insufficient to have a detectable impact on the large-scale, long term energy losses. As this paper is primarily focused on the identification of appropriate mixing models, it is proposed to adopt the value of $Re \approx 3,000$ as the laminar/non-laminar threshold. It is not essential to define the upper boundary for transitional turbulence, the critical zone, in this context, as the fully-turbulent Gaussian impulse response function has been shown to be applicable down to $Re \approx 3,000$.

Practical Implications

For turbulent and critical flow ($Re > 3,000$), a Gaussian impulse response function can provide a good estimate of the system's mixing characteristics that is effectively independent of the time after injection. However, previous work has suggested that the dispersion coefficients predicted by Taylor's expression (Equation 4) are only valid for highly turbulent flow, i.e. $Re > 20,000$. The present data has also confirmed the inapplicability of Taylor's estimate of the dispersion coefficient for $Re < 20,000$. Hence, an estimate of the dispersion coefficient that accounts for low-Reynolds Number effects for $Re < 20,000$ is required. Figure 9 illustrates a simple regression-based empirical expression for the variation of the dimensionless longitudinal dispersion coefficient for the new data presented here for Reynolds Number between 3,000 and 50,000, namely:

$$\frac{D_{xx}}{\bar{u}d} = 1.17 \times 10^9 Re^{-2.5} + 0.41 \quad (18)$$

The values predicted by Equation 18, for $10,000 < Re < 50,000$, are around twice the magnitude predicted by both Taylor (1954) and the results from Keyes (1955). As described earlier the experimental facilities and methods would suffer limitations. Taylor (1954) only provided three experimental values, in the range $10,000 < Re < 20,000$, two of which are above the variation predicted by Equation (4). The results from Keyes (1955) were obtained in air flow, employing a dynamic response method, from a sinusoidally modulated gas composition with frequencies between 3 and 10 cycles per second, within a 2.438 m long pipe. Longitudinal velocities of > 10 m/s were created and using a scanning rate of 1 cycle/min., the wave amplitude and phase were obtained, from which estimates of longitudinal mixing coefficients were made based on wave attenuation. In comparison, the new data presented here is the mean of three repeat solute tracer injections in water, directly measured over a 10 m length, with rapid response, non-intrusive instruments. The results show excellent mass balance and good repeatability, providing confidence in the results.

For laminar flow, the observed RTDs deviate significantly from symmetrical Gaussian distributions because the flow conditions – in either the laboratory or a real water main – are such that full mixing requires time periods far in excess of the time-scales of practical interest. As previously noted, the ADE can only describe the concentration profile once the solute is well mixed.

The present study suggests that the theoretical RTD for laminar flow proposed by Danckwerts (1953), the differential of Equation 12, provides a suitable model for laminar flow conditions. This expression provides a prediction of an RTD that is significantly different to the symmetrical Gaussian profile predicted by Taylor (1953) for laminar dispersion coefficient which requires dimensionless mixing time, $\tau > 0.5$ (equation 6). The crucial difference is that Danckwerts (1953) solution neglects the effect of molecular diffusion, and only accounts for the effects of differential advection caused by the parabolic laminar velocity profile. Hence, whereas Taylor's model assumes full cross-sectional mixing, Danckwerts (1953) model assumes no radial exchange, and thus should provide an improved approximation of the RTD at small times after injection, when there has been insufficient time for molecular diffusion to have led to any significant radial exchange. Figure 12 shows a comparison

between the experimentally-obtained CRTDs and Danckwerts (1953) theoretical CRTD for laminar flow. It can be seen that there is good agreement when $Re < 3,000$, confirming that a theoretical RTD assuming no radial exchange can provide a good approximation of the actual mixing characteristics of a system in the initial period, when $\tau < 0.5$.

Figure 13 compares recorded downstream temporal concentration distributions in laminar flow, shown in Figure 8e & f, with previously proposed predictions. Predictions employing the Lee (2004) and Romero-Gomez & Choi (2011) method have been made by routing the upstream profile, using mean dispersion coefficients determined from equation 9, with $\beta(t)$ evaluated from equation 10 & 11 respectively. In comparison, the recorded upstream profile has been convolved with the RTD from Danckwerts (1953). For $Re = 2670$ (Figure 13a), Taylor predicts a dispersion coefficient of $26.8 \text{ m}^2/\text{s}$ (not shown), with Lee (2004) predicting $0.23 \text{ m}^2/\text{s}$ and Romero-Gomez & Choi (2011) $0.05 \text{ m}^2/\text{s}$. For $Re = 1820$ (Figure 13b) the values are 12.45 , 0.16 and $0.04 \text{ m}^2/\text{s}$ respectively. This plot supports the finding of Romero-Gomez & Choi (2011) that the dispersion coefficient predicted by Lee (2004) over estimates observations of axial dispersion. Figure 13 also illustrates that for these very low dimensionless mixing times in laminar flow, the analytical RTD, which assumes no radial diffusion, can be convolved with the recorded upstream profile to provide predictions which are very close to the downstream data.

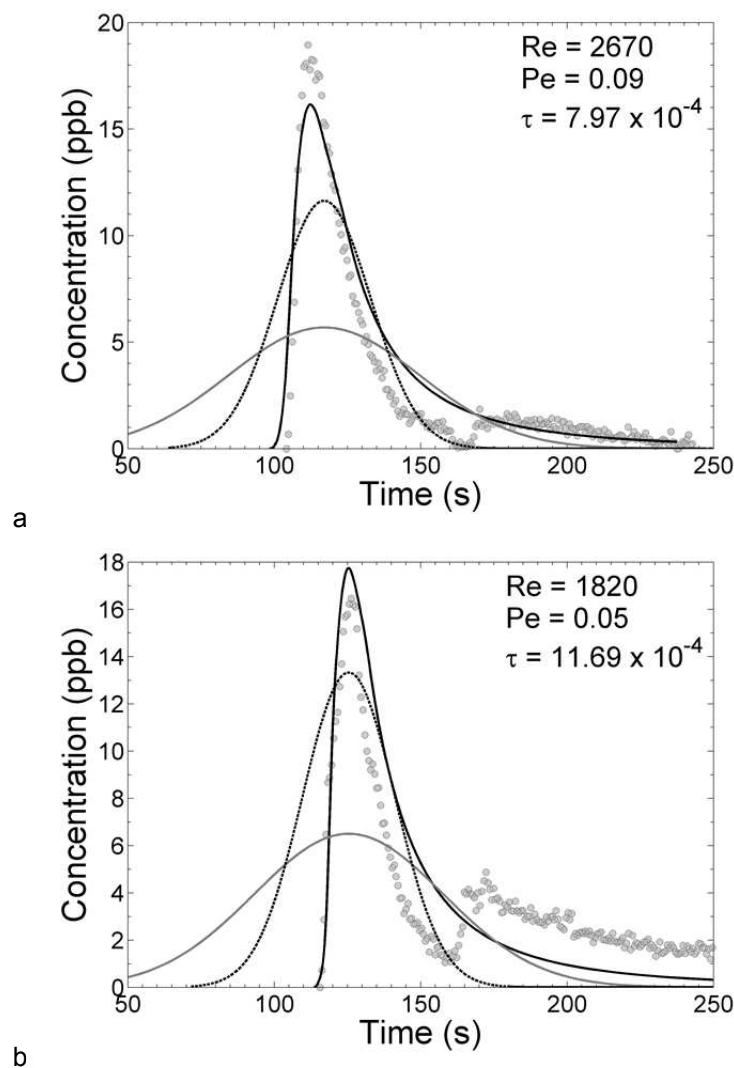


Figure 13 – Comparison between laboratory data (circles) and predictions from Lee (2004) (grey line), Romero-Gomez & Choi (2011) (dashed line) and Danckwerts (1953) CRTD (black line) for laminar flow.

Overall the results show that despite the complex hydraulics of turbulent, critical and laminar pipe flow for $2,000 < Re < 50,000$, the entire range can be described by just two impulse response functions. A Gaussian impulse response function provides a good description of the system's mixing characteristics for turbulent and critical flow for practically all times after injection. For most practical applications with laminar flow, where predictions

are required for scenarios when the solute has been in the flow for times of the order of minutes and hours, the RTD derived by Danckwerts (1953) provides a good estimation of the system's mixing characteristics.

Conclusions

Tracer data collected for a range of Reynolds Number covering turbulent, critical and laminar pipe flow were deconvolved to obtain the system's fundamental mixing responses or RTDs. Four main conclusions were made:

- For turbulent flow ($Re > 5,000$) the presence of turbulent diffusion means that the tracer becomes rapidly cross-sectionally well mixed, as such the system's mixing characteristics can be described by a Gaussian impulse response function, in practice for all times after injection.
- For critical flow ($3,000 < Re < 5,000$) the presence of transient turbulence is sufficient to rapidly mix the solute, and this range can also be described by a Gaussian impulse response function, independent of time since injection.
- For low Reynolds Number turbulent and critical flows, Taylor's (1954) equation does not provide a robust estimate of $\frac{D_{xx}}{\bar{u}d}$. An empirically-derived equation (18) for predicting $\frac{D_{xx}}{\bar{u}d}$ for $3,000 < Re < 50,000$ has been proposed.
- For laminar flow, the time for the solute to become well mixed is impractical for typical potable water distribution network pipe dimensions. However, it was shown that in the initial period $\tau < 0.5$, a theoretical RTD that assumes no radial exchange can be used to provide a good description of the system's mixing characteristics.

On the basis of these findings, RTD can be estimated for turbulent, critical and laminar pipe flow independently of the time after injection.

References

- Avila, K.; Moxey, D.; de Lozar, A.; Avila, M.; Barkley, D., and Hof, B. The onset of turbulence in pipe flow. *Science*, 333:192–196, 2011.
- Benedict, R. P. *Fundamentals of pipe flow*. John Wiley and Sons, 1980.
- Buchberger, S. G; Carter, J. T.; Lee, Y., and Schade, T. G. Random demands, travel times and water quality in deadends. *American Water Works Association Research Foundation*, Report 90963F:470, 2003.
- Danckwerts, P. V. Continuous flow systems distribution of residence times. *Chemical Engineering Science*, 2(1):1–13, 1953.
- Fischer, H. B. Longitudinal dispersion and turbulent mixing in open channel flow. *Annual Review of Fluid Mechanics*, 5:59-78, 1973.
- Flint, L. F. and Eisenklam, P. Longitudinal gas dispersion in transitional and turbulent flow through a straight tube. *The Canadian Journal of Chemical Engineering*, 47:101-106, 1969.
- Fowler, F. C. and Brown, G. G. Contamination by successive flow in pipe lines. *American Institute of Chemical Engineers*, 39:491-516, 1943.
- Gill, W. N. and Sankarasubramanian, R. Exact analysis of unsteady convective diffusion. *Proceedings of the Royal Society of London*, 316(1526):341–350, 1970.
- Guymer, I. and Stovin, V. R. One-dimensional mixing model for surcharged manholes. *Journal of Hydraulic Engineering*, 137(10):1160–1172, 2011.
- Hart, J. R. *Longitudinal dispersion in steady and unsteady pipe flow*. PhD thesis, The University of Warwick, 2013.
- Hart, J. R., Guymer, I., Jones, A., and Stovin, V. Longitudinal dispersion coefficients within turbulent and transitional pipe flow. In: Rowinski, Pawel, (ed.) *Experimental and Computational Solutions of Hydraulic Problems*. GeoPlanet: Earth and Planetary Sciences. Berlin, New York: Springer Berlin Heidelberg, 133-145: 2013.
- Hattersley, J. G., Evans N. D., Bradwell, A. R., Mead, G. P. and Chappell, M. J. Nonparametric prediction of free-light chain generation in multiple myelomapatients. 17th Int. Federation of Automatic Control World Congress (IFAC), International Federation of Automatic Control (IFAC), 8091–8096: 2008.
- Keyes, J. J. Diffusion film characteristics in turbulent flow: Dynamic response method. *American Institute of Chemical Engineers*, 1:305-311, 1955.
- Lee, Y. *Mass Dispersion in Intermittent Laminar Flow*. PhD thesis, University of Cincinnati, USA, 2004.
- Levenspiel, O. Longitudinal mixing of fluids flowing in circular pipes. *Industrial and Engineering Chemistry*, 50(2):343–346:1958.
- Madden, F. N; Godfrey, K. R.; Chappell, M. J.; Hovorka, R., and Bates, R. A. A comparison of six deconvolution techniques. *Journal of Pharmacokinetics and Biopharmaceutics*, 24(3):283–299, 1996.
- MATLAB [Computer software]. Natick, MA, MathWorks

- Moody, L. F. and Princeton, J. N. Friction factors for pipe flow Transactions of the ASME, 66:671-684, 1944.
- Romero-Gomez, P. and Choi, C. Y. Axial Dispersion Coefficients in Laminar Flows of Water-Distribution Systems, Journal of Hydraulic Engineering, 137(11), 1500-1508, 2011.
- Rutherford, J. C. *River Mixing*. John Wiley and Sons, 1994.
- Skilling, J. and Bryan, R. K. Maximum entropy image reconstruction general algorithm. *Monthly Notices of the Royal Astronomical Society*, 211:111–124, 1982.
- Sonnenwald, F.; Stovin, V. R., and Guymier, I. Configuring maximum entropy deconvolution for the identification of residence time distributions in solute transport applications. Journal of Hydrologic Engineering, 19(7):1413–1421, 2014.
- Stovin, V. R; Guymier, I. Chappell, M. J., and Hattersley, J. G. The use of deconvolution techniques to identify the fundamental mixing characteristics of urban drainage structures. *Water Science and Technology*, 61(8):2075–2081, 2010.
- Taylor, G. I. Dispersion of soluble matter in solvent flowing slowly through a tube. *Proceedings of the Royal Society*, 219(1137):186–203, 1953.
- Taylor, G. I. The dispersion of matter in turbulent flow through a pipe. *Proceedings of the Royal Society*, 223(1155):446–468, 1954.
- Tzatchkov, V. G.; and Li, Z. Buchberger, S. G., Romero-Gomez, P. and Choi, C. Axial dispersion in pressurized water distribution networks: A review. *International Symposium on Water Management and Hydraulic Engineering*, Ohrid, Macedonia, 1-5 September, 2009.
- White, F.M. Fluid Mechanics (7th ed.) McGraw-Hill, 2011.
- Young, P., Jakeman, A. and McMurtrie, R. An instrument variable method for model order identification. *Automatica*, 16, 281-294, 1980.